Geochemical characteristics and petrogenesis of the main granitic intrusions of Greece: an application of trace element discrimination diagrams

E. BALTATZIS,* J. ESSON† AND P. MITROPOULOS*

* University of Athens, Department of Geology, Panepistimiopolis, Ano Ilisia, Athens 15784, Greece

† University of Manchester, Department of Geology, Manchester M13 9PL, England

Abstract

Geochemical investigation of samples from 20 granitic intrusions in six tectonic zones of the Hellenides shows that both I-type and S-type granites occur in the region. The I-type granites from four of the zones, namely the Rhodope Massif (RM), the Serbomacedonian Massif (SMM), the Perirhodope Zone (PRZ) and the Attico-cycladic Zone (ACZ), show some systematic differences in their geochemistry. In particular, the Rb, Y, Nb, K and Ti contents increase in the sequence PRZ, SMM, RM and ACZ. The PRZ granites are of Jurassic age, those of the SMM and RM are Eocene to Oligocene and the ACZ ones are Miocene. The differences between zones are attributed to a combination of differences in partial melting and high-pressure fractionation processes. Geochemical differences within zones are explained by variable degrees of amphibole and apatite fractionation and accumulation.

KEYWORDS: granite, intrusion, geochemistry, trace elements, discrimination, Greece.

Introduction

VARIOUS granitic intrusions of Jurassic to Eocene age occurring in Greece, especially in Macedonia, Thrace and in some of the islands of the Aegean Sea (Fig. 1) have been studied previously. Most of the work has been mineralogical and petrological (e.g. Augustidis, 1972; Dürr *et al.*, 1978; Kokkinakis, 1980; Katerinopoulos, 1983; Kyriakopoulos, 1987) but some geochemical studies, mainly for major elements, have been carried out (e.g. Marinos and Petrascheck, 1956; Papadakis, 1965; Marakis, 1969; Andriesen *et al.*, 1979; Salemink, 1985) and, as described later, some radiometric dates have been reported.

The present comparative study of the major and trace element geochemistry was undertaken to investigate possible relationships between the tectonic setting and the principal granitic bodies in Greece. The results may prove useful in constraining models for the genesis of the granitic rocks and the associated mineralisation. The generic term 'granite' will be used in this paper for any plutonic rock containing more than 5% of modal quartz in accordance with the usage of Pearce *et al.* (1984) in their work on trace element discrimination diagrams as indicators of the tectonic environment.

Geological setting

The Hellenides along with the Dinarides form the Dinaric branch of the Alpine belt. The Hellenides are described in terms of ten 'isopic' zones flanked by two others, one to the south-west and the other to the north-east. The term 'isopic' zone has been widely used to refer to each successive zone with a distinctive facies succession. The major phases of sedimentation and orogenesis of the Hellenides can be related in a general way to the relative plate motion of Eurasia and Africa, documented by the spreading history of the North Atlantic (Smith, 1971; Dewey *et al.*, 1973; Channell and Horvath, 1976; Biju-Duval *et al.*, 1977).

Mountrakis (1983) distinguished the following isopic zones from east to west:

A. Rhodope massif (RM)

Mineralogical Magazine, December 1992, Vol. 56, pp. 487–501
© *Copyright the Mineralogical Society*

B. Serbomacedonian massif (SMM)
C. Perirhodopic zone (PRZ)
D. Axios (Vardar) zone (AZ) divided into: D1 Paeonias zone; D2 Paicon zone; D3 Almopias zone
E. Pelagonian zone (PZ)
F. Attico-Cycladic zone (ACZ)
G. Subpelagonian zone (SPZ)
H. Parnassos-Giona zone (PGZ)
I. Pindos zone (PNZ)
J. Gavrovo-Tripolis zone (GTZ)
K. Ionian zone (IZ)
L. Paxos zone (PXZ)

According to Brunn (1956) the above A–G isopic zones, forming the eastern part of the Hellenides, comprise the 'internal' belts, while the H–L isopic zones, forming the western part of the Hellenides, comprise the 'external' belts of the Hellenides. It is considered that the internal zones have been formed under 'inner arc' geotectonic conditions while the external zones have

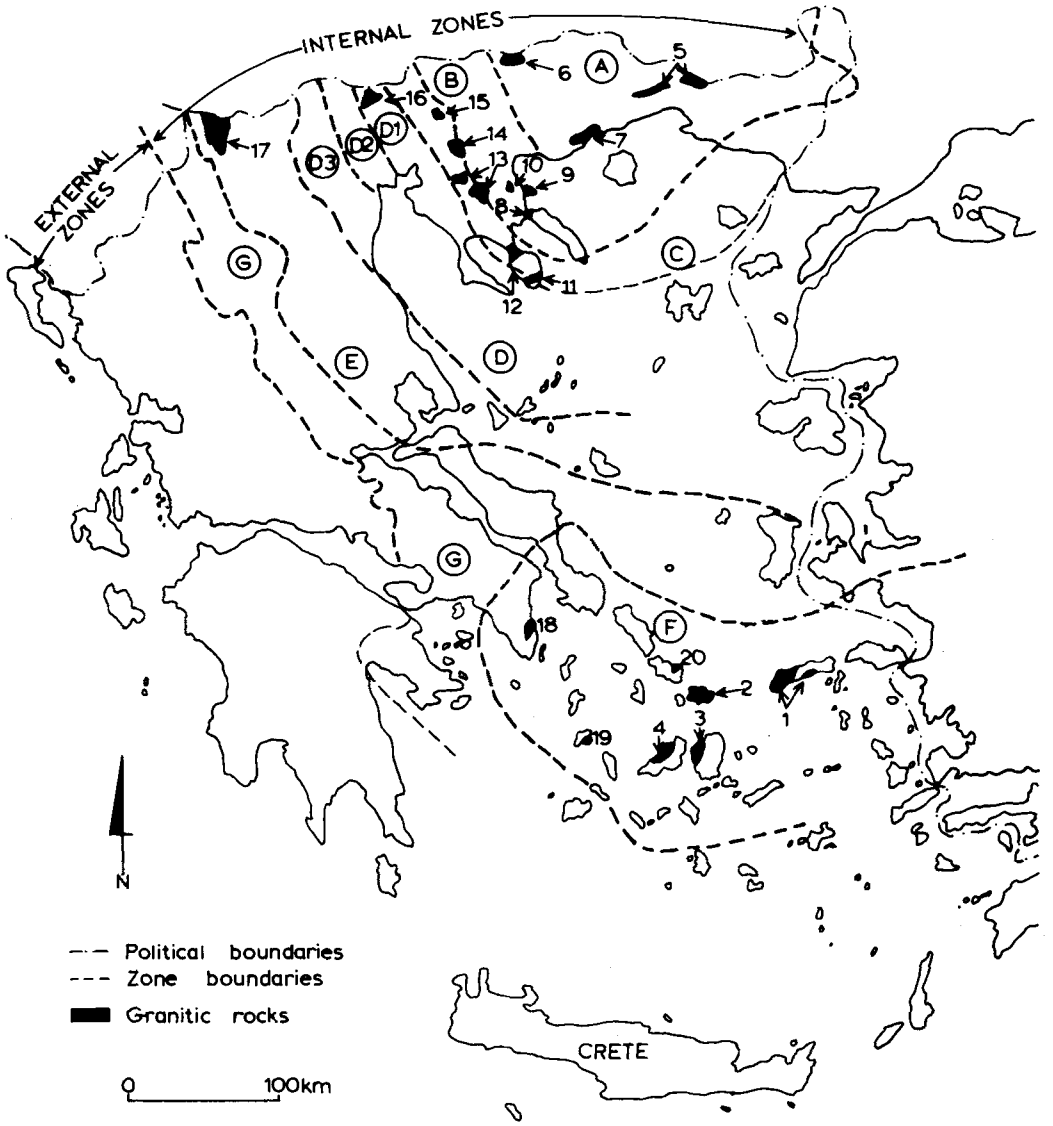

FIG. 1. Map showing the granitic intrusions sampled and relevant tectonic zones of the Hellenides. The key to the intrusion numbers is given in Table 1 and the tectonic zones are listed in the text.

Table 1. Key to granitic bodies in Fig. 1

Zone	Symbol on plots	Number on map	Name (abbreviation)
ACZ	•	1	Ikaria (IKR)
		2	Mykonos (MYK)
		3	Naxos (NX)
		4	Paros (PR)
		18	Laurium (LA)
		19	Serifos (SE)
		20	Tinos (TI)
RM	+	5	Xanthi (X)
		6	Vrodou (VR)
		7	Kavala (KB)
SMM	o	8	Ierissos (IE)
		9	Olympias (OL)
		10	Stratoni (ST)
PRZ	x	11	Toroni (TO)
		11	Sarti (SAR)
		11	Sykea (SYK)
		12	Ormos Panagias (ORP)
		13	Arnaea (AR)
		14	Sohos (SO)
		15	Nikopolis (NIK)
AZ	□	16	Fanos (FAN)
PZ	△	17	Florina (F)

been formed under 'outer arc' geotectonic conditions. As is shown in Fig. 1 (and Table 1) the major Greek granitic intrusions occur in the internal (A–G) isopic geotectonic zones.

A. Rhodope massif

This structural unit consists of a metamorphic basement of Hercynian age and older together with Mesozoic sediments; further deformation occurred during Alpine events. The granitic intrusions of Xanthi, Serres-Drama (of which the Vrodou granite forms a part) and Kavala occur in this zone. According to Kronberg (1966) the principal magmatic manifestations in the Rhodope massif happened during the last stages of the Alpine orogenic tectonic regime (Eocene–Oligocene–Miocene).

Xanthi. Augustidis (1972) describes this granite as a calc–alkaline body with biotite and hornblende; the same granite has been described by Christofides (1977). According to Meyer (1966) the age of the Xanthi granite is Oligocene and this is confirmed by Kronberg *et al.* (1970) who report ages of 27.4 ± 0.5 and 27.1 ± 0.4 Ma.

Serres-Drama. Papadakis (1965) describes the mineralogy and the petrology of the Serres-Drama granitic intrusion. K/Ar dating of hornblende yielded ages of 29 ± 1 and 33 ± 2 Ma for the Vrodou area of the granite (Marakis, 1969).

Kavala. This granite–granodiorite–diorite composite intrusion has been described by Kokkinakis (1980). The granitic rocks appear to have a complex thermal history or be the result of at least two periods of intrusive activity. Some of the rocks have a minimum age of Upper Carboniferous, but K/Ar dating on biotite yields an age of 17.8 ± 0.8 Ma for the youngest event. Recent Rb/Sr dating (Kyriakopoulos, 1987) yielded an age of 22.8 ± 2.4 Ma for the Kavala granite.

B. Serbomacedonian massif

This contains the granitic intrusions of Ierissos, Olympias and Stratoni. The Stratoni–Olympias area consists mainly of gneisses, amphibolites, mica schists, marbles and phyllites. K/Ar dates of 108–114 Ma on amphiboles from amphibolite (Harre *et al.*, 1968) are assumed to represent a real phase of metamorphism of Aptian to Barremian date, but it is likely that earlier events affected some parts of the zone. In addition, almandine–amphibolite facies metamorphism of upper Palaeocene to lower Oligocene data is indicated by K/Ar and Rb/Sr dates on gneissose rocks (56 to 34 Ma; Harre *et al.*, 1968). The above-mentioned metamorphic rocks are ultrabasic rocks. The granitoid intrusions of Stratoni, Olympias and Ierissos are associated with massive sulphide mineralisation. K/Ar dating on biotite of the Stratoni granodiorite yielded an age of 29.6 ± 1.4 Ma (Dürr *et al.*, 1978). Harre *et al.* (1968) reported K/Ar and Rb/Sr ages of 22–48 Ma for granitic rocks in this zone.

C. Perirhodopic zone

Most of the rocks in this zone are Mesozoic marine sediments, variably deformed and metamorphosed by Alpine events. The main granitic intrusions are those of Sarti–Sykea–Toroni, Ormos Panagias, Arnaea, Sohos and Nikopolis.

Marakis (1969) reported a K/Ar age of 140 ± 3 Ma for the Nikopolis (Lachana) granite, while Jurassic ages for the granites of Arnaea and Sarti–Sykea have been deduced from stratigraphic criteria (Dürr *et al.*, 1978).

D. Axios zone

This zone consists mainly of sediments of Mesozoic and Tertiary age; the only granite is at Fanos, within the Paeonias division of the Axios zone. This granite has been intruded within gabbros of the ophiolite complex of the Geugeli area. Borsi *et al.* (1964), using Rb/Sr and K/Ar dating, found that it has an age of 150 ± 2 Ma, which Marakis (1969) has confirmed with a K/Ar age of 148 ± 4 Ma.

E. Pelagonian zone

The Florina granite consists of two main bodies intruded into a Hercynian metamorphic basement (Dercourt, 1964) consisting of sericitic gneisses and schists. K/Ar dating of biotites yielded a model age of 460 Ma for the older, deformed intrusion and 240 Ma for the younger, undeformed intrusion (Marakis, 1969).

F. Attico–Cycladic zone

The Cycladic islands are part of a belt of crystalline complexes linking continental Greece with the Menderes massif in Turkey. The Attico–Cycladic complex consists of at least two main tectonic units (Dürr *et al.*, 1978). The lower unit is formed by a sequence of thrust sheets made up of a pre-Alpidic basement, Mesozoic marbles, metavolcanites and metapelites. The upper unit consists of various Klippen comprising ophiolitic material, Permian sediments and high-temperature metamorphic rocks. Mineral assemblages within the lower unit indicate a polymetamorphic history:

(*a*) a high-pressure, blueschists facies metamorphism (M1), which has been dated in the middle Eocene (*c.* 42 Ma; Altherr *et al.*, 1979; Andriessen *et al.*, 1979);
(*b*) a medium-pressure metamorphism (M2), which has been dated around the Oligocene–Miocene boundary (20–25 Ma; Altherr *et al.*, 1979; Andriessen *et al.*, 1979);
(*c*) the intrusion of granitoid magmas, which took place immediately after the second metamorphic phase (22–14 Ma; Altherr *et al.*, 1982).

Altherr *et al.* (1982) reported that the plutons now exposed on several islands (Ikaria, Naxos, Paros, Mykonos, Serifos, Tinos) and in Laurium, exhibit a systematic regional variation in composition with increasing K_2O values from southwest to northeast.

Ikaria. The western part of the island consists of a cataclastic leucogranite (sample IKR-1), while sample IKR-2 represents a slightly deformed granite in the SE. The western body gives K/Ar and Rb/Sr ages of 8.2–9.0 Ma, while the most reliable ages for the south-eastern granite are 9.2–10.7 Ma (Dürr *et al.*, 1978; Altherr *et al.*, 1928).

Naxos. This island is essentially composed of a metamorphic complex and a granodioritic mass. On Naxos the glaucophane schist facies (M1) is dated at 40 to 50 Ma while the late Oligocene–Miocene Barrovian type overprint reached its peak at *c.* 25 Ma (Andriessen *et al.*, 1979). The metamorphic complex, a migmatitic gneiss dome surrounded by a sequence of metamorphic zones, is a metasedimentary–metavolcanic sequence mainly composed of interbedded mica schists and marbles. The western part of Naxos consists of a granodioritic intrusion with a tourmaline-rich aplitic border facies representing the latest stage of crystallisation. The granodioritic intrusion caused local low-*P*–high-*T* metamorphism. After its consolidation the granodioritic mass was severely affected by deformation (Jansen and Schuiling, 1976; Jansen, 1977). Rb/Sr isochrons obtained from samples of the granodiorite gave ages of 11.7 ± 0.8 and 11.1 ± 0.7 Ma (Dürr *et al.*, 1978; Andriesen *et al.*, 1979).

Paros. The western neighbour of Naxos consists of a sequence of migmatites, gneisses, schists and marbles and some granitic intrusions which have been variably deformed (Philippson, 1959). From the medium-pressure/high-temperature mineral assemblages which occupy the islands of Paros, only cooling ages (K–Ar, Rb–Sr and fision track), ranging from 15 to 7 Ma have been reported for hornblende, muscovite, biotite, apatite and titanite (Wendt *et al.*, 1977). The granites of Paros are thought to be of Miocene age (Dürr *et al.*, 1978) and Altherr *et al.* (1982) report ages of 11.4–12.4 Ma for the micas.

Mykonos. Two main tectonic units can be distinguished. The lower one is formed by a granodiorite intrusion and sparse remnants of the country rocks. The upper unit has only been preserved as Klippen (Dürr and Altherr, 1979). K/Ar dating of biotite from the granodiorite yielded a model age of 10.0 ± 3 Ma (Dürr *et al.*, 1978) and Marakis (1973) reported a K/Ar age of 12.0 ± 0.9 Ma, also for biotite. Altherr *et al.* (1982) report K/Ar and Rb/Sr ages of 10.1–12.0 Ma for the granodiorite, some from minerals and others from whole rocks.

Serifos. On this island a granodiorite is

intruded into a series of metasediments (Salemink, 1985), affected by a late Oligocene–Miocene Barrovian type metamorphism (Andriessen *et al.*, 1979). The granodiorite and the country rock are cut by numerous dykes of dacitic to rhyolitic composition. The granodiorite has been dated by the K/Ar method, giving 9.2 ± 0.4 Ma for hornblende and 8.3 ± 0.2 Ma for biotite (Dürr *et al.*, 1978); these ages agree with the 8.6–9.5 Ma reported by Altherr *et al.* (1982).

Tinos. Melidonis (1980) divided the metamorphic rocks of Tinos into two subunits of high-*P*/low-*T* metamorphic rocks. Age determinations (Rb–Sr and K–Ar) on white micas from these rocks yielded ages of about 40 Ma while for medium-*P*/high-*T* metamorphic rocks, only cooling ages (K–Ar, Rb–Sr and fission track) ranging from 15 to 7 Ma have been reported (Wendt *et al.*, 1977). During a later low to medium-*P*/*T* metamorphism granitic magma was intruded and caused intensive contact metamorphism. Rb/Sr and K/Ar ages from minerals and whole rocks date the granite at 14.0–15.4 Ma (Altherr *et al.*, 1982).

Laurium. According to Marinos and Petrascheck (1956) two tectonic subunits can be distinguished in southern Attica. A granodiorite intruded into both units near the village of Plaka, causing contact metamorphism (Marinos and Petrascheck, 1956). Data, including P–T-X_{CO_2} stability relations, for a calc–silicate hornfels from the Plaka area reveal that it has been metamorphosed at temperatures between 440 and 600 °C in a H_2O-rich fluid with a low partial pressure of CO_2 (Baltatzis, 1981). K/Ar ages reported for the granodiorite are 8.8 ± 0.5 Ma for a whole rock (Dürr *et al.*, 1978) and 8.3 ± 0.11 Ma for biotite (Altherr *et al.*, 1982).

Sampling and analytical techniques

Samples representing the most typical rock types of each major granitic intrusion were collected. In Table 2, the locality, texture,

Table 2. List of analysed samples and their mineralogy.

Zone	Sample no.	and rock type	Principal minerals
ACZ	IKR1	Slightly deformed coarse granite	Q, A, Ab72-77, B
	IKR2	Microgranite, slight lineation/schistosity	Q, A, Ab70-85, B, M
	MYK	Granodiorite	Q, A, Ab50-65, B, H, P
	NX1	Coarse granodiorite, slight lineation	Q, A, Ab54-69, B, H
	PR1	Microgranite, slight lineation	Q, A, Ab76-79, B, M
	LA	Granodiorite	Q, A, Pl, B, H*
	SE	Granodiorite	Q, A, Pl, B, H
	TI	Granodiorite	Q, A, Pl, B, H
RM	X1,2	Coarse granodiorite	Q, A, Ab50-80, B, H
	VR3,5	Granodiorite	Q, A, Ab60-77, B, H
	KB1	Diorite, slight schistosity	Q, Ab49-63, B, H
	KB2	Diorite	Q, Ab45-67, B, H
	KB3	Granodiorite	Q, A, Ab60-80, B, H
	KB4	Granodiorite	Q, A, Ab55-78, B, H*
	KB5	Granitic gneiss	Q, A, Ab80-100, M
SMM	IE1	Granite	Q, A, Ab77-84, B
	OL1	Leucogranite	Q, A, Ab82-84, B
	OL2	Granodiorite	Q, A, Ab70-80, B, H*
	ST1,2	Granodiorite	Q, A, Ab59-70, B, H
PRZ	TO	Granodiorite	Q, A, Ab71-80, B, H*
	SAR1	Granodiorite, slight lineation	Q, A, Ab65-77, B, H
	SYK	Granodiorite	Q, A, Ab75-85, B, H
	ORP1,2	Granite, slight lineation	Q, A, Ab76-88, B, M
	AR1,2	Coarse leucogranite	Q, A, Ab98-100, M
	SO1,2	Plagiogranite	Q, Ab100, M
	NIK	Coarse granite	Q, A, Ab71-75, B
AZ	FAN1,2	Leucogranite	Q, A, Ab78-87, B
PZ	F7,11	Q syenite/K-metasom. granodiorite	Q, A, Pl*, B, H

Q = quartz, A = alkali feldspar, B = biotite, H = hornblende, M = muscovite, P = pyroxene, Pl = plagioclase of undetermined composition; Ab compositions determined by electron microprobe; * indicates a phase showing a high degree of alteration.

mineralogy and rock type of each analysed sample is given. The mineralogy was determined by optical microscopy and electron microprobe analysis using a Cambridge Instrument Geoscan fitted with a Link Systems model 290-2KX energy-dispersive spectrometer and ZAF-4/FLS quantitative analysis software system. The samples were analysed for major and trace elements by X-ray fluorescence analysis using a Philips PW 1450 spectrometer; details of the technique used and the correction procedures involved have been described by Brown *et al.* (1973).

Geochemical characteristics

The major and trace element results and the CIPW norms of the analysed rock samples are given in Table 3. All the analysed granitic rocks except those of Arnaea and Sohos and the sample KB5 from Kavala show I-type calc–alkaline mineralogical chemical properties. The granites of Arnaea and Sohos (samples AR1,2,SO1,2) are clearly of S-type as in these two granites muscovite is the only mica present, the plagioclase is albite (Ab_{98-100}) rather than andesine to oligoclase as in the other granites (Table 2), the CaO contents are low (0·09–0.32 wt.%) and the Rb/Sr ratios are high (3–11). Both granites also have molar $Al_2O_3/(CaO + alkalis)$ ratios in excess of 1.1 giving normative corundum up to 3.8% (Table 3). Sample KB5 from the Kavala granite also shows most of the S-type characteristics listed above, while the other four samples from the Kavala pluton (KB1–4 inclusive) are clearly of I-type.

The I-type granites have normative An contents below 12 wt.%, the granodiorites contain 15–21 wt.% and the diorites greater than 22%. The S-type granites have the highest normative Q (34–38%) and lowest An (0–2% plus one sample with 3.7%) contents of all the samples studied.

The plot of TiO_2 against Zr (Fig. 2*a*) shows a positive linear relationship for most of the samples. The Kavala pluton (Rhodope massif), however, shows very little variation in Zr (200–220 ppm) but has a range of TiO_2 values. TiO_2 and Zr, except for Zr in the Kavala samples, decrease as SiO_2 increases.

On the Sr against Zr plot (Fig. 2*b*) there are three distinct distributions: (*a*) the S-type granites of Arnaea and Sohos can be clearly identified by their very low Sr contents; (*b*) the ACZ samples lie close to a line with a slope of 1.6; (*c*) most of the samples from the PRZ and the SMM and some of those from the RM, are distributed around a line with a slope of 1.6; (*c*) most of the samples from the PRZ and the SMM and some of those from the RM, are distributed around a line with a steeper slope 5. As in the case of TiO_2, the Sr contents decrease as SiO_2 increases.

Fig. 3 shows the mantle normalised large ion lithophile and high field strength element plots (Wood *et al.*, 1979) for the most acid granite sample from each of the isopic tectonic zones. It is clear from this diagram that all of the samples show typical geochemical characteristics, i.e. high LIL/HFS element ratios, negative Nb anomalies, etc, of calc–alkaline granite associated with the subduction of oceanic lithosphere beneath island arc systems and continental margins (Plant *et al.*, 1985).

Figs. 4, 5 and 6 show the results plotted on some of the diagrams used by Pearce *et al.* (1984) for the discrimination of oceanic ridge granites (ORG), within-plate granites (WPG), volcanic arc granites (VAG) and collision granites (COLG). These plots are also useful for displaying the variation in granitic rocks between and within the tectonic zones of Greece.

The ORG normalised geochemical diagrams for the granitoid samples from the ACZ, RM, SMM, PZ and the I-type samples from the PRZ (Fig. 4*a–d*) have shapes similar to the plots of typical VAG (Pearce *et al.*, 1984), especially those of the Jamaican intrusive rocks (Isaacs, 1975). They are characterised by enrichments of K, Rb and Ba relative to Nb, Ce, Zr and Y, normalised Zr and Y values less than unity and an overall trend of intermediate steepness which, together with the absence of a negative Ba anomaly, is typical of VAG.

The RM samples have a quite narrow range and their field is plotted on each part of Fig. 4 to aid comparison of one zone with another. Relative to the RM, the I-type samples of the PRZ (Fig. 4*a*) exhibit a wider compositional range and contain lower levels of K, Rb and Y. The S-type granites (SO and AR) of the PRZ have patterns which differ significantly from those of the I-type bodies in this tectonic zone; the Arnaea granite has much much lower Ba contents, and somewhat higher K, Rb, Nb and Y contents, than its I-type counterparts, while the Sohos granite is only distinguished in this plot by its higher Y content. Samples from the ACZ have patterns similar to those from the RM (Fig. 4*b*) but the former show a greater range of composition. Apart from one sample with lower Nb, Ce, Zr and two samples with lower Y, the SMM rocks (Fig 4*c*) plot within or very near the RM field.

The close similarity between the RM, ACZ and SMM samples in Fig. 4 suggests that the granitic rocks in these three zones were generated by

similar evolutionary paths from sources of similar composition. In the case of the RM and SMM, adjacent zones with contemporaneous (late Eocene to early Miocene) intrusive activity, the likenesses are not unexpected. However, granites with similar trace element fingerprints were produced in the ACZ, during the middle to late Miocene, 10–20 Ma later and some 300 km to the south, inferring that source materials of similar mineralogy and incompatible element contents existed on this time-scale beneath both the south Aegean region and the area adjacent to the north Aegean.

Samples of the Florina granitoid, in the PZ, plot at the top of, or just above, the RM field but the shapes of the PZ and RM patterns are virtually identical (Fig. 4*d*). This implies that the source material for the very much older (Palaeozoic) PZ magma had an incompatible element fingerprint essentially indistinguishable from that of the source of the RM magmas.

The pattern for the only granite (Fanos) in the AZ (Fig. 4*d*) has a steeper overall trend than those of the I-type granitic rocks of all the other zones. This is a consequence of the high Rb and Nb, but low Zr and Y, contents of the Fanos samples; another notable feature is its low Ba content. In terms of the incompatible elements, the only similarities between the AZ granite and the granitic rocks of the same age (Middle to Late Jurassic) in the adjacent PRZ are the Ce and Y contents. These differences between the AZ and PRZ granitic rocks are probably due to the greater degree of fractional crystallisation involved in the evolution of the former rather than significant differences between their respective sources. Other chemical properties of the AZ granite, when compared with those of the PRZ support this hypothesis: their low P_2O_5, TiO_2 and Sr contents (Table 3 and Figs 2 and 3); their high SiO_2 and low MgO and CaO (Table 3).

The variation of the K/Rb ratio between zones can be illustrated by reference to Fig. 4. Differences in slope of the lines K–Rb show that relative to the RM the granitic rocks of the PRZ have higher K/Rb ratios, while the ACZ and SMM samples have K/Rb ratios close to those of the RM ones. In the case of the AZ the K/Rb ratios are much lower than in the neighbouring PRZ but this is probably the effect of different amounts of fractional crystallisation, as suggested above.

In the Y–SiO_2 diagram (Fig. 5) all samples except that the Arnaea granite lie well within the VAG + COLG field as a consequence of their low Y contents, a feature which has been noted above in the discussion of Fig. 4. Y shows a general decrease as SiO_2 increases, with similar but well defined separate trends being shown by the samples from the PRZ (I-type rocks) the ACZ and the SMM, while the RM samples show little variation of Y and SiO_2. The S-type granites from the PRZ are clearly distinguished by their high Y contents; in contrast, the I-type rocks of the PRZ exhibit the lowest Y–SiO_2 trend of all the Greek tectonic zones.

In the Rb–(Y + Nb) diagram (Fig. 6), which Pearce *et al.* (1984) found to have more discriminating power than the two-element plots, none of the samples plot in the COLG field. Apart from the S-type granites from Arnaea, the only samples which plot just outside the VAG field boundary in Fig. 6 are three from the ACZ and one from the PZ. This is due to their (Y + Nb) contents being only 1–4 ppm, i.e. 2–8% relative, above values which would plot on the boundary. However, the ACZ is, from geological criteria, clearly a volcanic arc environment; thus boundaries of such diagrams should be regarded as useful guidelines rathe than immutable.

As in the Y–SiO_2 diagram (Fig. 5) the Rb–(Y + Nb) plot (Fig. 6) shows well defined pseudo-linear trends, with similar slopes, for the I-type samples from the PRZ, SMM and ACZ. SiO_2 contents increase from right to left along each of these trends, i.e. within each of the zones PRZ. SMM and ACZ higher Rb values are associated with higher SiO_2 contents. At a given value of (Y + Nb) the Rb contents increase in the sequence PRZ, SMM and ACZ, the same sequence as in the Y–SiO_2 plot. In contrast to the trends within these three zones, the RM samples form a cluster as they show little variation in Rb or (Y + Nb) despite the large SiO_2 range of samples from the RM.

Discussion and conclusions

In terms of the criteria of Pearce *et al.* (1984), all except one of the Greek granites studied here have the geochemical characteristics of granites generated in a volcanic arc environment. The samples of the Arnaea granite plot in the WPG field in Figs. 5 and 6 due mainly to their high Y and slightly high Nb contents. As this granite is one of several of Jurassic age in the PRZ, there is no geological evidence that it was generated in a different tectonic environment from the others in this zone. Thus, we conclude that its distinguishing geochemical characteristics are due to its source material, discussed below, rather than its tectonic environment.

I-type granitic rocks from the four tectonic zones, ACZ, RM, SMM and PRZ, in which most Greek granites occur show some small but

Table 3. Chemical composition of granitic rocks from Greece (major elements and CIPW norms in wt%, trace elements in ppm)

Zone	A C Z								R M									S M M		
Rock No	IKR1	IKR2	MYK	NX1	PR1	LA	SE	TI	X1	X2	VR3	VR5	KB1	KB2	KB3	KB4	KB5	IE1	OL1	OL2
SiO_2	73.07	70.68	66.82	67.82	69.52	68.93	67.79	69.08	65.63	65.84	64.98	66.45	56.42	57.46	68.21	67.55	72.27	70.16	72.62	68.92
TiO_2	0.31	0.26	0.62	0.63	0.32	0.46	0.61	0.46	0.49	0.49	0.38	0.38	0.72	0.67	0.27	0.26	0.27	0.28	0.06	0.47
Al_2O_3	13.95	16.10	15.61	14.71	16.45	16.10	15.60	15.45	16.29	16.19	16.81	16.24	16.78	17.08	16.57	16.89	15.01	15.74	15.40	15.57
Fe_2O_3	0.17	0.41	0.34	0.63	0.00	1.18	1.35	1.20	1.47	1.33	1.45	1.33	2.58	2.81	1.09	0.79	1.07	0.95	0.48	0.11
FeO	1.51	1.02	2.67	2.54	1.58	1.31	1.50	1.33	1.80	1.87	1.84	1.70	4.69	4.07	1.11	1.36	0.84	0.77	0.38	2.67
MnO	0.01	0.01	0.01	0.03	0.01	0.01	0.02	0.02	0.04	0.04	0.03	0.03	0.10	0.08	0.03	0.04	0.01	0.01	0.02	0.02
MgO	0.87	0.83	1.44	1.50	0.67	1.00	1.54	1.11	1.58	1.56	1.24	1.19	3.71	3.27	1.05	1.04	0.80	0.90	0.15	1.14
CaO	1.64	1.86	4.17	3.95	2.01	3.23	3.94	3.17	3.92	3.90	4.43	3.79	6.71	6.35	3.41	3.60	2.75	2.35	1.04	3.58
Na_2O	3.03	4.13	2.97	2.45	3.79	3.25	2.97	3.30	3.50	3.44	3.62	3.59	3.35	3.48	4.05	4.15	2.82	4.34	3.83	3.40
K_2O	4.76	4.15	4.07	4.34	4.58	3.38	3.15	3.52	4.22	4.23	4.11	4.35	2.78	2.76	3.19	3.37	4.78	3.35	5.66	2.51
P_2O_5	0.10	0.12	0.23	0.23	0.12	0.14	0.16	0.14	0.19	0.18	0.21	0.20	0.20	0.20	0.15	0.14	0.12	0.15	0.04	0.18
LOI	0.62	0.58	0.80	0.79	0.82	0.90	1.20	1.10	0.57	0.60	0.85	0.73	1.39	1.20	0.75	0.65	1.22	0.96	0.39	1.11
Total	100.05	100.14	99.75	99.62	99.88	99.88	99.83	99.86	99.69	99.67	99.95	99.98	99.43	99.43	99.89	99.84	99.96	99.95	100.07	99.67
Nb	13	8	20	28	12	25	25	19	12	12	7	13	10	12	9	8	11	16	3	12
Zr	134	140	305	236	179	210	206	171	206	207	174	180	211	213	209	216	149	167	73	239
Y	18	15	28	29	15	27	29	23	22	25	15	17	27	26	19	20	21	8	10	20
Sr	197	236	450	418	222	418	298	300	379	371	741	456	642	630	683	751	137	500	292	254
Rb	191	206	167	201	241	101	101	162	187	181	143	167	136	138	127	134	181	124	153	112
Th	31	38	57	55	46	38	50	59	41	41	38	49	85	83	52	48	62	40	12	49
Pb	3	8	7	8	5	6	8	9	8	8	8	18	32	38	7	8	3	7	19	10
Ni	13	14	15	9	9	4	5	7	4	8	9	8	17	18	7	8	3	6	4	14
Cr	27	28	33	32	22	29	39	33	23	23	45	23	31	32	26	23	22	32	26	31
Ce	36	42	87	81	47	50	49	46	72	62	38	47	52	58	53	52	57	60	21	58
Nd	15	19	37	41	20	24	23	15	30	28	21	24	34	23	24	23	29	21	3	26
V	17	8	21	25	2	21	22	8	52	48	62	50	138	122	24	26	10	21	6	32
La	32	19	59	29	25	-	-	-	49	33	24	36	22	30	32	30	36	28	10	32
Ba	280	456	712	570	607	742	550	450	718	731	766	727	565	567	784	901	818	546	446	715
Sc	7	8	10	13	6	7	13	6	12	15	12	8	18	19	7	6	9	7	3	10
Qtz	31.43	25.08	22.01	25.55	23.53	28.77	27.88	28.04	18.45	18.89	17.08	19.08	6.20	8.15	23.24	20.63	34.69	25.66	26.10	28.30
Cor	0.84	1.44	0.00	0.00	1.60	1.56	0.52	0.79	0.00	0.00	0.00	0.00	0.00	0.00	0.26	0.00	3.85	0.71	1.09	0.74
Or	28.13	24.50	24.04	25.62	27.08	20.00	18.60	20.78	24.91	25.02	24.32	25.70	16.43	16.29	18.83	19.90	28.25	19.78	33.44	14.84
Ab	25.65	34.91	25.10	20.74	32.06	27.46	25.12	27.91	29.62	29.10	30.62	30.41	28.37	29.43	34.27	35.14	23.82	36.71	32.45	28.79
An	8.13	9.22	17.29	16.35	9.99	15.09	18.51	14.82	16.29	16.25	17.47	15.35	22.54	22.87	16.94	17.51	3.72	11.64	5.14	17.76
Di	0.00	0.00	2.80	2.66	0.00	0.00	0.00	0.00	2.52	2.48	3.66	2.80	8.73	7.01	0.00	0.27	0.00	0.00	0.00	0.00
Hy	4.31	3.19	5.81	5.56	4.07	3.20	4.51	3.50	4.08	4.29	2.92	3.08	10.47	8.94	3.36	3.96	2.22	2.43	0.61	6.89
Mt	0.25	0.60	0.49	0.92	0.00	1.71	1.96	1.74	2.14	1.92	2.10	1.92	3.74	4.07	1.59	1.15	1.56	1.38	0.70	0.15
Ilm	0.59	0.49	1.19	1.21	0.60	0.87	1.71	0.87	0.93	0.93	0.72	0.72	1.37	1.28	0.51	0.49	0.51	0.53	0.11	0.90
Hm	0.00	0.00	0.00	0.00	0.00	0.00	0.00	0.00	0.00	0.00	0.00	0.00	0.00	0.00	0.00	0.00	0.00	0.00	0.00	0.00
Ap	0.23	0.26	0.53	0.53	0.28	0.32	0.37	0.32	0.44	0.41	0.48	0.46	0.46	0.46	0.34	0.32	0.27	0.34	0.09	0.41

Table 3. (cont

Zone	--- S M M ----		---------- P R Z ----------					----- A Z ----					----- P Z ----	
Rock No	ST1	ST2	TO	SAR1	SYK	ORP1	ORP2	AR1	AR2	SO1	SO2	NIK	FAN1	FAN2	F7	F11
SiO_2	64.01	61.71	67.96	61.69	67.28	72.36	72.03	75.30	76.06	76.00	74.86	67.57	75.06	74.56	67.19	65.41
TiO_2	0.41	0.42	0.35	0.55	0.30	0.24	0.24	0.24	0.14	0.19	0.21	0.61	0.13	0.13	0.43	0.40
Al_2O_3	17.12	16.64	16.65	17.25	17.11	15.38	15.73	13.31	13.08	13.40	14.25	16.07	13.63	14.09	15.26	16.69
Fe_2O_3	1.54	0.64	1.06	1.38	0.67	0.54	0.62	1.17	0.82	0.82	1.26	0.38	0.53	0.71	1.72	1.73
FeO	1.95	3.05	1.17	2.77	1.38	0.72	0.71	0.26	0.37	0.49	0.40	2.64	0.40	0.22	1.10	1.49
MnO	0.04	0.04	0.01	0.04	0.02	0.00	0.01	0.00	0.00	0.00	0.00	0.01	0.00	0.00	0.05	0.04
MgO	1.84	1.75	1.32	2.35	1.13	0.53	0.53	0.35	0.24	0.45	0.64	1.04	0.23	0.16	1.58	1.62
CaO	4.16	5.00	3.06	5.53	3.62	1.90	2.14	0.09	0.32	0.21	0.16	2.49	0.67	0.65	2.47	2.05
Na_2O	3.33	3.10	4.52	4.53	4.68	4.19	4.25	3.34	4.04	4.37	4.38	3.52	3.54	3.53	3.61	3.26
K_2O	3.90	3.16	2.89	1.93	2.69	3.41	3.16	5.37	4.42	3.26	2.74	4.37	5.49	5.67	5.48	5.35
P_2O_5	0.21	0.23	0.21	0.40	0.25	0.10	0.10	0.03	0.03	0.04	0.03	0.30	0.04	0.02	0.31	0.24
LOI	1.24	3.87	0.87	1.20	0.78	0.67	0.69	0.61	0.58	0.92	1.18	0.87	0.33	0.36	0.62	1.53
Total	99.74	99.61	100.08	99.62	99.91	100.02	100.20	100.06	100.10	100.14	100.10	99.87	100.05	100.09	99.82	99.81
Nb	6	6	13	14	13	5	3	22	33	10	10	15	32	38	15	27
Zr	193	198	194	257	209	163	164	203	142	180	200	195	94	96	215	221
Y	20	19	10	13	9	7	6	59	70	43	39	26	11	8	25	28
Sr	690	665	651	916	777	350	429	17	31	23	25	152	96	163	474	409
Rb	141	127	103	69	79	115	97	189	163	79	81	142	286	263	150	227
Zn	62	53	49	67	41	50	46	6	29	11	14	51	4	3	35	40
Cu	72	69	4	6	8	3	2	1	14	8	10	3	6	3	6	8
Ni	10	12	12	21	15	4	5	8	6	8	7	7	8	6	16	27
Cr	31	33	25	44	28	21	20	24	21	23	22	29	22	22	41	46
Ce	67	69	53	69	68	50	35	89	82	51	58	89	46	44	71	71
Nd	27	31	23	29	25	23	18	29	43	25	29	36	14	14	26	35
V	53	65	36	53	24	7	7	8	5	7	10	38	9	8	36	40
La	38	35	30	46	42	34	25	25	42	33	40	42	41	29	41	49
Ba	737	702	905	626	1065	646	644	119	72	462	608	589	149	312	840	1056
Sc	12	16	5	18	7	5	4	8	5	8	6	9	4	7	10	11
Qtz	17.38	16.82	21.74	12.60	19.66	29.87	29.67	34.62	34.61	37.00	37.62	21.87	31.65	30.72	18.23	18.85
Cor	0.00	0.00	0.52	0.00	0.00	1.35	1.44	1.85	1.08	2.30	3.80	1.03	0.66	0.98	0.00	1.82
Or	23.05	18.69	17.11	11.39	15.89	20.13	18.66	31.72	26.15	19.26	16.18	25.84	32.46	33.51	32.36	31.60
Ab	28.16	26.19	38.25	38.29	39.63	35.47	35.97	28.26	34.16	36.97	37.04	29.78	29.94	29.85	30.53	27.58
An	20.25	22.18	15.20	21.08	17.72	9.41	10.59	0.44	1.58	1.03	0.78	12.34	3.31	3.21	9.29	10.16
Di	0.30	2.17	0.00	5.17	0.20	0.00	0.00	0.00	0.00	0.00	0.00	0.00	0.00	0.00	2.32	0.00
Hy	6.12	7.73	3.29	6.45	4.24	1.79	1.72	0.87	0.59	1.11	1.60	6.14	0.65	0.40	2.86	4.76
Mt	2.23	0.93	1.54	2.01	0.98	0.78	0.90	0.15	0.80	1.02	0.68	0.55	0.76	0.32	2.47	2.50
Ilm	0.79	0.80	0.66	1.05	0.57	0.45	0.45	0.45	0.26	0.36	0.39	1.17	0.25	0.25	0.81	0.77
Hm	0.00	0.00	0.00	0.00	0.00	0.00	0.00	1.07	0.27	0.11	0.79	0.00	0.00	0.49	0.01	0.00
Ap	0.48	0.53	0.48	0.92	0.57	0.23	0.23	0.07	0.07	0.09	0.07	0.69	0.09	0.05	0.71	0.55

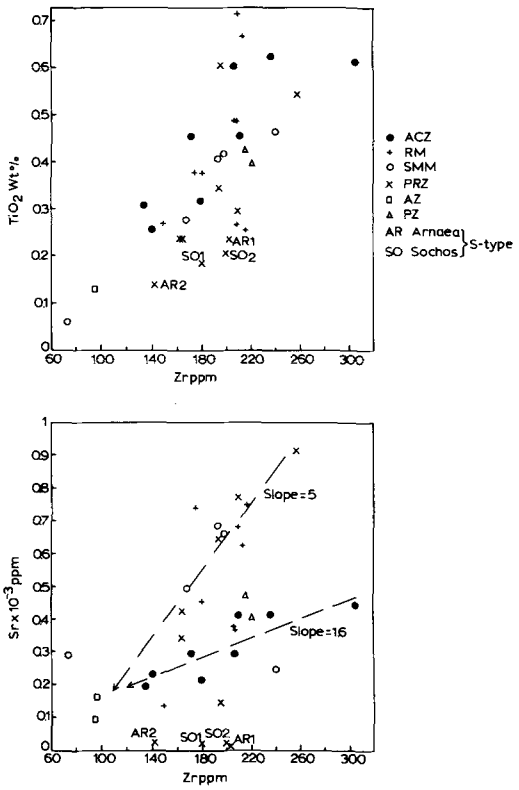

FIG. 2. (*a*) TiO_2–Zr plot. (*b*) Sr–Zr plot. SiO_2 increases in the direction of the arrows.

systematic differences in their trace element geochemistry. The differences, both between and within zones, are best displayed in Y–SiO_2 (Fig. 5) and Rb–(Y + Nb) (Fig. 6) diagrams. Despite some scatter around the trend for each zone, it can be seen from Fig. 6 that, at a given (Y + Nb) content, there is a progressive increase by a factor of 1.5–1.6 in the Rb content from one zone to another in the sequence PRZ, SMM and ACZ. At a given SiO_2 value the Y concentrations increase by a similar factor (1.6–1.8) in the same sequence (Fig. 5). The PRZ granites are clearly distinguishable by their lower Rb and Y contents (Figs 3–6) from those of the RM, SMM and ACZ. For the I-type samples from each of these zones the mean Rb and Y values increase in the sequence PRZ, SMM, RM and ACZ, the values being 101, 131, 155 and 171 ppm for Rb and 11.8, 15.4, 21.3 and 23.0 ppm for Y. The mean (Y + Nb) values show the same trend (22.3, 24.0, 31.7 and 41.8), despite the fact that the mean Nb values, 10.5, 8.6 and 10.4 ppm respectively, for the PRZ, SMM and RM samples show little variation and the ACZ samples have a much higher mean Nb content of 18.8 ppm.

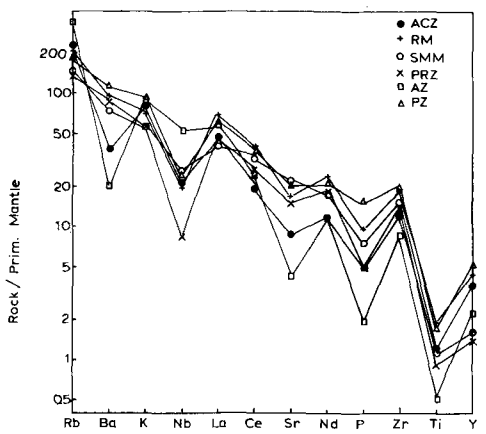

FIG. 3. Mantle-normalised plot (after Wood *et al.*, 1979) of the most acid I-type granite from each tectonic zone.

According to the model proposed by Pearce *et al.* (1984) the Rb and (Y + Nb) contents of volcanic arc granites are controlled by a sequence of processes, the effects of which are illustrated in Fig. 7. Model evolutionary paths were described by Pearce *et al.* for the granites of Alaska (points with subscript A) and central Chile (subscript C); there are four principal stages.

1. Selective introduction of Rb, together with other LIL elements, from the subduction zone into the overlying mantle; this process, represented by enrichment from M_A to E_A and from M_C to E_C, has little effect on Y and Nb due to their retention in the subducted slab.
2. Partial melting of the LIL-enriched mantle to leave a harzburgitic residue; this results in enrichment of Rb, Y and Nb, together with other incompatible elements, in the primary melts P_A and P_C.
3. High-pressure fractionation of olivine, plagioclase and augite, causing further enrichment of the incompatible elements, to produce evolved basic magmas B_A and B_C.
4. Fractionation of plagioclase, clinopyroxene, amphibole, magnetite and, at a later stage, biotite to produce intermediate (I_A and I_C) and acid (A_A and A_C) magmas; during this process Rb continues to be enriched in the evolving liquid but the fractionation of amphibole, magnetite and accessory phases prevent further enrichment, and can even cause some depletion of Y and Nb.

Examination of Fig. 7 shows that it is the mantle composition and stage 1 which are the largest factors influencing the differences in the Rb contents of the evolved liquids, although

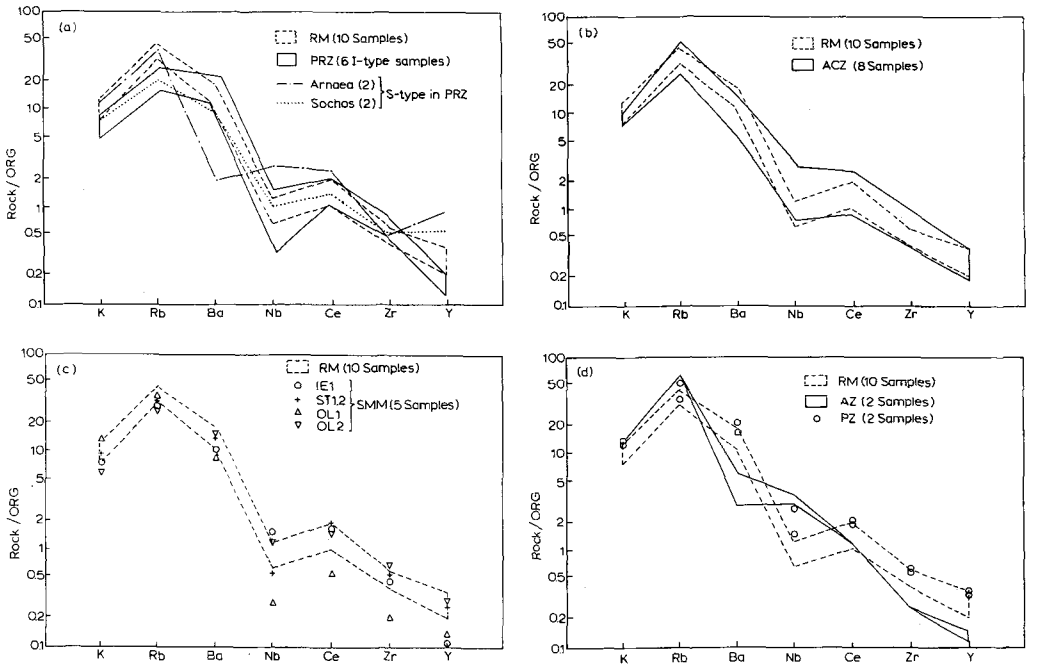

FIG. 4. Ocean ridge granite normalised plots (after Pearce *et al.*, 1984). All samples from each tectonic zone plot within the relevant outlined area and the field for the Rhodope Massif is shown on all diagrams to facilitate comparison. The S-type granites are identified separately.

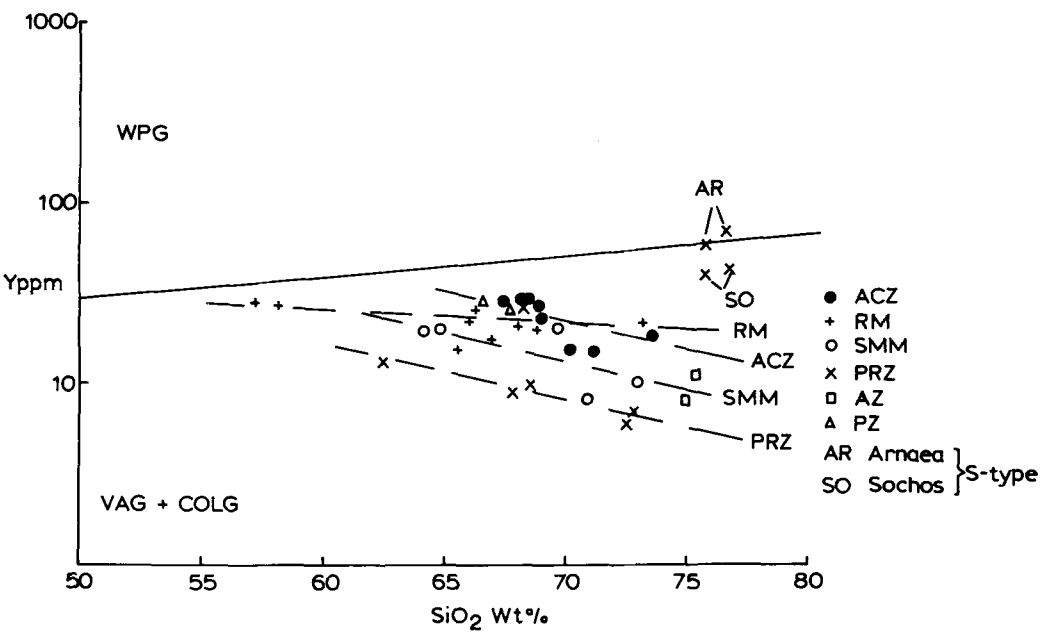

FIG. 5. Y–SiO_2 plot. The lines are to assist identification of general trends within zones.

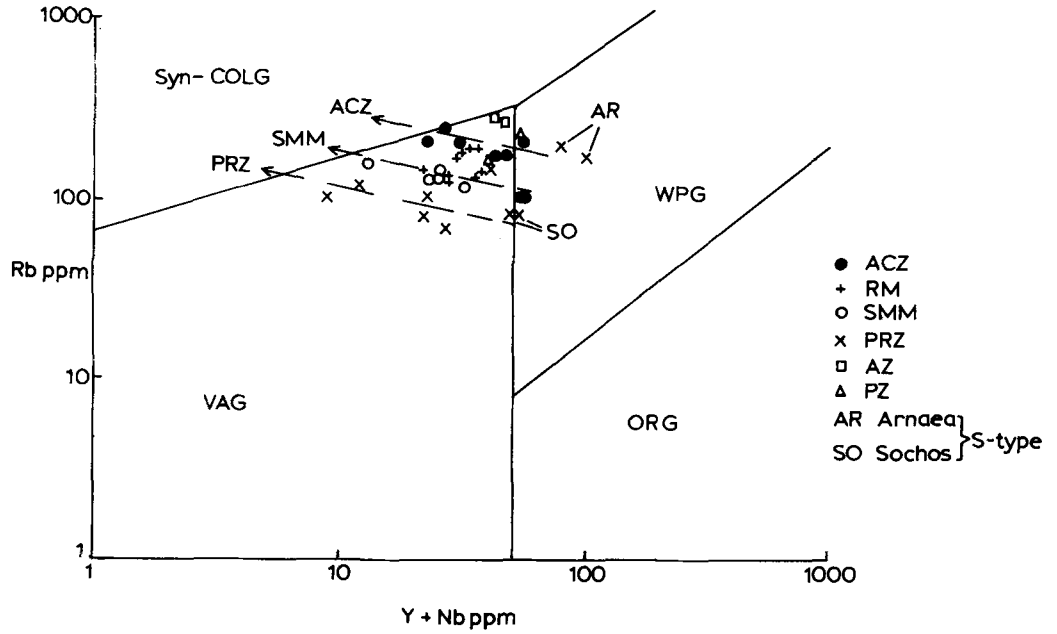

FIG. 6. Rb–(Y + Nb) plot. The lines are to assist identification of general trends within zones; SiO_2 increases in the direction of the arrows.

variations in the proportions of phases fractionating during stage 4 will also have a significant effect. Values of (Y + Nb) are thought to show little variation in the mantle due to the narrow range of Y contents and the low abundance of Nb relative to Y. If this is correct, then it is stages 2 and 3 which will have the greatest influence on the (Y + Nb) contents of the residual acid magmas but during stage 4 fractionation of significant amounts of hornblende or accessory minerals and, to some extent biotite, clinopyroxene or magnetite (see mineral vectors on Fig. 7) will also have an appreciable effect.

The simplest explanation of the variation of Rb and Y + Nb within the granites of central Chile is that they evolved by several paths involving different degrees of partial melting, stage 2, and different amounts of high-pressure fractionation, stage 3, so that a number of basic magmas, lying along the line P_CB_C and its extrapolation, with different Rb and (Y + Nb) contents were produced prior to the low-pressure fractionation, stage 4, which gave rise to the acid end-products. This mechanism would account for the distribution of the rocks about a line almost parallel to P_CB_C. The Alaskan granites have an almost circular field, suggesting that, relative to those of Chile, their evolution involved little variation in the factors, mainly stages 2 and 3, controlling (Y + Nb) contents and somewhat greater variation in the factors, mainly mantle composition and stages 1 and 2, controlling Rb contents.

Within the Greek granites studied here, there is considerably greater variation than is the case for central Chile and Alaska (Fig. 7). Consider first variation within the zones PRZ, SMM and ACZ; in each case the samples lie close to lines compatible with the fractionation of hornblende and accessory minerals from magmas of intermediate to acid composition. This mechanism is supported by the fact that the samples plotting nearest to the left-hand end of each trend (Figs 6 and 7) contain biotite as the only ferromagnesian mineral, while the other samples contain both biotite and hornblende (Table 2) and greater amounts of apatite. Further support is provided by other geochemical differences within each zone; from right to left along each trend P_2O_5, CaO, MgO and total Fe decrease and SiO_2 increases. Thus we conclude that the chemical variation within each of these three zones is due mainly to fractionation and accumulation of hornblende and apatite. Separation of these phases will produce liquids to the left of the median points and their accumulation will give compositions to the right. In the case of the RM and PZ samples, which contain biotite and hornblende, there is no petrographic or geo-

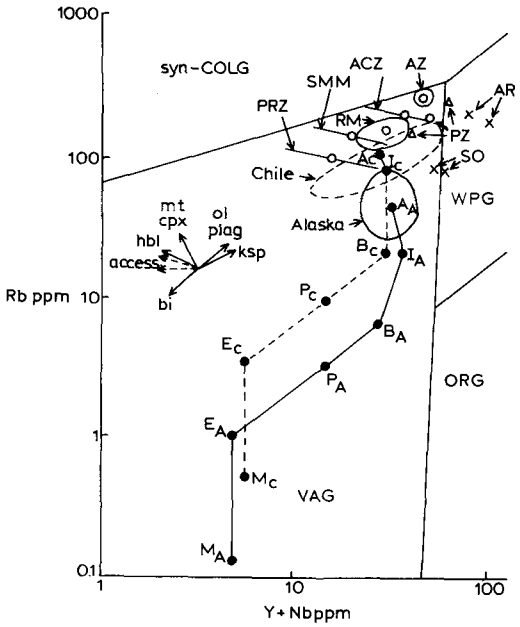

FIG. 7. Rb–(Y + Nb) diagram showing the Pearce *et al.* (1984) model paths of magma generation and evolution of volcanic arc granites from central Chile and Alaska, together with the distribution (summarised from Fig. 6) of granites from the different tectonic zones of Greece. Small circles mark the median values for samples from each tectonic zone; the remaining legend is described in the text. The directions of liquid composition trends due to mineral fractionation from intermediate to acid magmas are indicated.

chemical evidence of significant fractionation of hornblende or apatite; if these zones show any trends at all, they resemble small-scale versions of the Chilean one. The AZ samples contain biotite but no hornblende and there is no evidence of fractionation within the granite; there are no known hornblende granites in this zone, but some could be present below the surface.

We now turn to consideration of the differences between the zones PRZ, SMM, RM, ACZ and AZ. The median points (represented by circles in Fig. 7) for the samples in each zone shown an alignment along a direction parallel to P_CB_C, suggesting that the differences between them are a consequence of different evolutionary histories during stages 2 and 3, i.e. during partial melting and the subsequent high-pressure fractionation, and that the granites in each zone have evolved from basic magmas with slightly different contents of Rb and (Y + Nb). If there had been significant differences between the LIL element compositions of the mantle sources beneath each zone, then the sense of variation between zones in Fig. 7 would be mainly vertical, i.e. like the difference between Alaska and Chile. The median points for the Greek tectonic zones lie within a field of size and orientation similar to that of the Chilean granites, indicating that similar petrogenetic histories were involved. The slightly higher Rb contents of the Greek granites could be due to their mantle source being slightly more enriched in Rb than the Chilean mantle.

We conclude that the Greek I-type granites evolved from mantle sources, with little compositional variation between zones, containing about twice as much Rb as the Chilean mantle. The differences between zones are due mainly to small variations in the degrees of partial melting and high-pressure fractionation, while differences within zones are the consequence of variable amounts of hornblende and apatite fractionation and accumulation at a late stage in the petrogenesis.

The Greek granites with S-type characteristics, AR and SO in the tables and figures, are closely similar to each other in their Si, Ti, Zr, P, Al, Fe, V, Ca and Sr contents (Table 3). However the AR and SO intrusions differ so much in Rb, K, Nb, Y, *REE*, Mg, Na and Ba that they must have quite different petrogenetic histories; the first five of these constituents are 1.5–2.7 times more abundant in AR than in SO, while Mg, Na and Ba are higher in SO by factors of 2, 1.2 and 5 respectively. Relative to their I-type counterparts in the PRZ with similar SiO_2 contents, the AR and SO granites have high Y (by a factor of 6–10), Nb (factor 2–7) and *REE* (factor 1.5–2) and low P (factor 0.3), Ca (factor 0.1), Sr (factor 0.07) and Zn (factor 0.3); in addition, the AR samples have low Mg (factor 0.5) and Ba (factor 0.16) but high K (factor 1.5) and Rb (factor 1.8).

These geochemical differences between the AR and SO granites, and between them and the other high-SiO_2 granites, are too complex to be explained merely by variations in the fractionation or abundances of accessory minerals. The absence of hornblende in these two intrusions and the above discussion of Fig. 7 show clearly that their high Y contents are incompatible with them being related to any of the other granites by processes involving hornblende fractionation. In addition, none of the types of hydrothermal alteration satisfactorily account for the positions, relative to the other high-SiO_2 granites, of AR and SO in Fig. 7 (see alteration trends in Fig. 8*a* of Pearce *et al.*, 1984). Thus we conclude that, taken as a whole, the differences between the AR and SO granites and the others are so significant that they are most likely to reflect major source differences.

The SO granite contains abundant quartz, albite (An_{100}) and muscovite (25–30%) but no K-feldspar, so that muscovite plagiogranite is a more appropriate name than granite. The AR granite contains less muscovite (*c.* 10%) and major K-feldspar in addition to quartz and albite. Such muscovite-rich assemblages cannot be produced directly from an igneous source but the muscovite could be the result of alteration of K-feldspar. However, in these intrusions there is no petrological evidence, i.e. no partly altered K-feldspar, for this process. Also, the muscovites of AR and SO contain about 7% total iron oxide and thus cannot be the product of simple alteration of K-feldspar. All of these factors lead us to suggest that the AR and SO magmas were produced by partial melting of non-igneous sources or are the result of major contamination, by this type of crustal material, of I-type magmas. Quartzofeldspathic schists containing major muscovite would be suitable candidates because (*a*) they are common in the area; (*b*) they have appropriate melting relations (Thompson, 1982; Le Breton and Thompson, 1988) for the generation of appreciable amounts of melt at reasonable temperatures (650–750 °C) and pressures (4–6 kbar); (*c*) the geochemistry of such rocks is compatible with that of the AR and SO intrusions. We attribute the differences between AR and SO to differences in the composition, and/or the degree of involvement, of their S-type components.

Acknowledgements

The constructive comments of an anonymous referee are acknowledged. The authors also thank Mr. V. Vergenakis for drawing all the figures for the paper.

References

Altherr, R., Schliestedt, M., Okrusch, M., Seidel, E., Kreuzer, H., Haare, W., Lenz, H., Wendt, I., and Wagner, G. A. (1979) Geochronology of high-pressure rocks on Sifnos (Cyclades, Greece). *Contrib. Mineral. Petrol.*, **70**, 245–55.

—— Kreuzer, H., Wendt, I., Lenz, H., Wagner, G., Keller, J., Harre, W., and Hohndorf, A. (1982) A late Oligocene/early Miocene high-temperature belt in the Attic–Cycladic Crystalline Complex (SE Pelagonian, Greece). *Geol. Jahrb.*, **E23**, 97–164.

Andriesen, P. A. M., Boelrijk, N. A. I. M., Hebeda, E. H., Priem, H. N. A., Verdurmen, E. A. Th., and Verschure, R. H. (1979) Dating the events of metamorphism and granitic magmatism in the Alpine orogene of Naxos (Cyclades, Greece). *Contrib. Mineral. Petrol.*, **69**, 215–25.

Augustidis, S. (1972) On the petrogenetic and geochemical relationship of the Mo–Cu–W–Bi hydrothermal quartz veins and the Fe–Cu–W–Mo epidote–garnet skarn bodies (contact metasomatism) of the younger intrusive granite of Kimmeria (Xanthi, Greece). *Scient. Annivers. Technic. Univ. of Athens*, **2**, 233–44.

Baltatzis, E. (1981) Contact metamorphism of a calc-silicate hornfels from Plaka area, Laurium, Greece. *Neues Jahrb Mineral., Mh*, 481–8.

Biju-Duval, B., Dercourt, J., and Le Pichon, X. (1977) From the Tethys Ocean to the Mediterranean seas: a plate tectonic model of the evolution of the western Alpine system. In *International Symposium on the History of Mediterranean Basins* (Split, Yugoslavia) (B. Biju-Duval and L. Montadert, eds). *Technip, Paris*, 143–64.

Borsi, S., Ferrara, G., and Mercier, J. (1964) Determination de l'age des series metamorphiques de massif Serbo-Macedonien au nord-est de Thessalonique (Grece) par les methodes Rb/Sr et K/Ar. *Ann. Soc. Geol. Nord.*, **84**, 223–5.

Brown, G. C., Hughes, D. J., and Esson, J. (1973) New XRF data retrieval techniques and their application to U.S.G.S. standard rocks. *Chem. Geol.*, **11**, 223–9.

Brunn, J. H. (1956) Contribution a l'etude geologique du Pinde septentrional et d'une partie de la Macedoine occidentale. *Ann. Geol. Pays Hellen.*, **7**, 246 pp.

Channell, J. E. T. and Horvath, E. (1976) The African/Adriatic promontory as a palaeogeographical premise for Alpine orogeny and plate movements in the Carpatho–Balkan region. *Tectonophysics*, **35**, 71–101.

Christofides, G. (1977) *Contribution to the study of plutonic rocks of the Xanthi area.* Ph.D. Thesis, Univ. of Thessaloniki (unpubl.).

Dercourt, J. (1964) Contribution a l'etude geologique d'un secteur du Peloponnese septetrional. *Ann. Geol. Pays Hellen.*, **15**, 1–418.

Dewey, J. F., Pitman, W. C., Ryan, W. B. F., and Bonnin, J. (1973) Plate tectonics and the evolution of the Alpine system. *Geol. Soc. Am. Bull.*, **84**, 3137–80.

Dürr, S. and Altherr, R. (1979) Existence des klippes d'une nappe composite neogene dans l'ile de Myconos (Cyclades, Grece). *Rapp. Comm. Int. Mer. Medit.*, **25/26** 2a, 33- Monaco.

—— Keller, J., Okrusch, M., and Seidel, E. (1978) The median Aegean crystalline belt: Stratigraphy, structure, metamorphism, magmatism. In *Alps, Appenines, Hellenides* (Closs, H., Roeder, D. H., and Schmidt, K., eds), 455–77.

Harre, W., Kockel, F., Kreuzer, H., Lenz, H., Muller, P., and Walther, H. W. (1968) Uber Rejuvenationen im Serbo-Mazedonischen Massiv (Deutung radiometrischer Altersbestimmungen). *Intr. Geol. Congress, 23*, **6**, 223–36.

Isaacs, M. C. I. (1975) *Comparative geochemistry of selected Jamaican intrusive rocks.* M.Sc. Thesis, Univ. of Leeds (unpubl.).

Jansen, J. B. H. (1977) The geology of Naxos. *Geol. and Geophys. Res.*, **19**, No. 1, IGME, Athens, 1–100.

—— and Schuiling, R. D. (1976) Metamorphism of Naxos: Petrology and geothermal gradients. *Am. J. Sci.*, **276**, 1225–53.

Katerinopoulos, A. E. (1983) *Contribution to the study of plutonic rocks of W. Varnoudas*. Ph.D. Thesis, Univ. of Athens (unpubl.).

Kokkinakis, A. (1980) Altersbesiehungen zwischen metamorphosen mechanischen deformationen und intrusionen am südrand des Rhodope-Massivs (Makedonien, Griechenland). *Geol. Rundschau,* **69**, 726–44.

Kronberg, P. (1966) Petrographie und tektonik im Rhodopen–Kristallin des Tsal Dag, Simvolon und Ost-Pangaon (Griechisch–Makedonien). *Neues Jahrb. Geol. Palaont., Mh.*, **7**, 410–24.

—— Meyer, W., and Pilger, A. (1970) Geologie der Rila–Rhodope–Masse zwischen Strimon und Nestos (Nord Griechenland). *Beih. Geol. Jahrb.*, **88**, 133–80.

Kyriakopoulos, K. G. (1987) *Geochronological, geochemical and mineralogical study of some Tertiary plutonic rocks of the Rhodope massif and their isotopic characteristics*. Ph.D. Thesis, Univ. of Athens (unpubl.).

Le Breton, N. and Thompson, A. B. (1988) Fluid-absent (dehydration) melting of biotite in metapelites in the early stages of crustal anatexis. *Contrib. Mineral. Petrol.*, **99**, 226–37.

Marakis, G. D. (1969) Geochronology studies of some granites from Macedonia. *Ann. Geol. Pays Hell.* **21**, 121–52.

—— (1973) Datations de roches des zones internes de la Grece. *C.R. des Seances de la Soc. Phys. et l'Histoire Natur. de Geneve*, **7**, 52–8.

Marinos, G. P. and Petrascheck, W. E. (1956) Laurium. IGME, *Geol. Geophys. Studies*, IV, No. 1.

Melidonis, N. (1980) The geological structure and mineral deposits of Tinos island (Cyclades, Greece). *The geology of Greece,* **13**, 1–80 (Greek with English summary).

Meyer, W. (1966) Alterseinstufung von Tektonik und Metamorphose des Rhodopen-Kristallins im Bos Dag (Griechisch-Ostmazedonien). *Neues Jahrb. Geol. Palaeont., Mh.*, **7**, 399–409.

Mountrakis, D. M. (1983) *Structural geology of the North Pelagonian zone and the geotectonic evolution of the internal zones of the Hellenides (Macedonia, Greece)*. Docent Thesis, Univ. of Thessaloniki (unpubl.).

Papadakis, A. (1965) *The plutonite of Serres-Drama*. Ph.D. Thesis, Univ. of Thessaloniki (unpubl.).

Pearce, J. A., Harris, N. B. W., and Tindle, A. J. (1984) Trace element discrimination diagrams for the tectonic interpretation of granitic rocks. *J. Petrol.*, **25**, 956–83.

Philippson, A. (1959) *Das Aegaeische Meer und seine Inseln*. Klosterman, Frankfurt.

Plant, J. A., O'Brien, C., Tarney, J., and Hurdley, J. (1985) Geochemical criteria for the recognition of high heat production granites. In *High heat production (HHG) granites, hydrothermal circulation and ore genesis*. Inst. Mining and Metall., London, 263–85.

Salemink, J. (1985) Skarn and ore formation at Seriphos, Greece. *Mededelingen van het Instiunt voor Aardwetenschappen der Rijksuniversiteit te Utrecht*, No. 40.

Smith, A. G. (1971) Alpine deformation and the oceanic areas of the Tethys, Mediterranean and Atlantic. *Geol. Soc. Am. Bull.*, **82**, 2039–70.

Thompson, A. B. (1982) Dehydration melting of pelitic rocks and the generation of H_2O-undersaturated granitic liquids. *Am. J. Sci.*, **282**, 1567–95.

Wendt, J., Raschka, H., Lenz, H., Kreuzer, H., Hohndorf, A., Harre, W., Wagner, G. A., Keller, J. Altherr, R., Okrusch, M., Schliestedt, M., and Seidel, E. (1977) Radiometric dating of crystalline rocks from the Cyclades (Aegean Sea, Greece). *Fifth European Coll. of Geochron. Cosmochron. and Isotope Geol., Pisa.* (vol. of abstracts).

Wood, D. A., Joron, J.-L., Treuil, M., Norry, M., and Tarney, J. (1979) Elemental and Sr isotope variations in basic lavas from Iceland and the surrounding ocean floor. *Contrib. Mineral. Petrol.*, **70**, 319–39.

[*Manuscript received 18 May 1990: revised 29 January 1992*]